© by PSP Volume 26 – No. 2a/2017, pages 1745-1755 Fresenius Environmental Bulletin

DIGITAL TERRAIN CHARACTERIZATION AND INTERPRETATION OF LAKE VAN REGION FOR EARTHQUAKE VULNERABILITY COMBINING REMOTE SENSING AND GEOGRAPHICAL INFORMATION SYSTEMS

Ali Can Demirkesen[1], Fatih Evrendilek[2,*]

[1]Department of City & Regional Planning, Izmir Institute of Technology, Izmir, Turkey
[2]Department of Environmental Engineering, Abant Izzet Baysal University, Turkey

ABSTRACT

The Lake Van basin and its surroundings (36,500 km^2) in the eastern Turkey have not been investigated adequately in terms of earthquake vulnerability, and pre-earthquake preparedness. In this study, a digital terrain model (DTM) of the Lake Van region was developed combining an ASTER digital elevation model (DEM), Landsat-7 ETM+ imagery, remote sensing techniques, and geographical information systems. Terrain characteristics derived from DTM with DEM, and a 3-D land-use and land-cover fly-through view such as fault zones, drainage patterns, lineaments, and landforms were interpreted in terms of earthquake vulnerability. Our results indicate that the directions of Mus-Tatvan (Mus thrust), Bitlis thrust, and Ercis-Patnos-Malazgirt-Varto-Karliova along with Van and Ercis possess the highest risk of earthquake hazards.

KEYWORDS:
Earthquake vulnerability; Geomorphological characterization; Digital terrain interpretation; Digital terrain model

INTRODUCTION

A total of 151 natural disasters such as earthquakes, epidemics, extreme heat waves, flood, slides, storms, and wild fires occurred in Turkey from 1900 to 2011 and caused the loss of 91,431 human lives, and the economic damage of 25 billion USD, adversely affecting 8,902,008 people [1]. Out of the 151 natural disasters, earthquake alone was the most frequent natural disaster (73 events) and was responsible for 97%, 92%, and 77% of the total human losses, and total economic and social damages, respectively [1]. Korkmaz (2009) reported that 90% of the buildings across Turkey are subject to the risk of earthquake disaster [2]. The earthquake event between Van and Ercis occurred on 23 October 2011 and was of the moment magnitude (M_w) 7.2 at a depth of about 10 km according to such institutions as the National Earthquake Monitoring Center of Bogazici University, the Kandilli Observatory and Earthquake Research Institute (KOERI), the Earthquake Engineering Research Center of the Middle East Technical University, and the Earthquake Engineering and Disaster Management Institute of Istanbul Technical University. The earthquake released its energy by the push-movement on the east-west trending fault line of about 50 to 100 km in length just to the east of Lake Van.

The KOERI indicated that although the epicenter is located at the North Anatolian fault zone, the fault suggests that the earthquake event belongs to the Bitlis-Zagros fault zone, where thrust mechanisms dominate along the border between the Anatolian and the Arabian tectonic plates. Both Van and Ercis are located along the shores of Lake Van where the existing soil liquefaction enhanced ground motions, thus causing collapses of buildings. Continuous sequences of aftershocks as of 23 October 2011 many of which were greater than M_w 4.0 shook the area severely and forced people to abandon their homes. Impacts of this earthquake hazard included losses of human lives, properties, and economic livelihood, migration as refugees, collapses of infrastructures and buildings, lack of shelter, food, medical care, clothing, and provision of public services such as utilities, communication systems, transportation, and schools.

The Lake Van region is under the first degree earthquake zone according to the earthquake and fault maps of Turkey. Earlier studies about historical background of earthquakes, seismicity, geological structures, fault zones, and soil and rock conditions of the Lake Van basin in the eastern Turkey reported that a great number of earthquakes with M_w of 4.0 to 7.3 occurred in the Lake Van basin for decades [3–9]. In spite of these reports, the Lake Van basin and its surroundings have been claimed not to be analyzed adequately in terms of earthquake vulnerability, pre-earthquake emergency prepa-redness, and pre-earthquake measures so far. Characterization of vulnerabilities is of vital

importance as the first step towards disaster-resilient societies [10]. Therefore, the objective of this study was to characterize earthquake vulnerability of the Lake Van region combining geographical information systems (GIS) and remote sensing (RS) techniques. In so doing, a digital terrain model (DTM) with a 3-D fly-through view of landscape topography and terrain characteristics such as drainage patterns, geological lineaments, digital elevation model (DEM), and land-use and land-cover (LULC) types was devised using the Advanced Space-borne Thermal Emission Reflection (ASTER) and Landsat-7 Enhanced Thematic Mapper Plus (ETM+) imageries in order to assist in the process of decision-making towards pre-earthquake preparedness and measures.

MATERIALS AND METHODS

Study region description. The Lake Van basin and its surroundings as our study region (36,500 km^2) are located in the eastern Turkey, surrounded by the provinces of Van in east, Bitlis in west, and Agri in north and possess a geological structure with erosion-induced tectonic plateaus, volcanic formations, caldera complexes, and fertile agricultural soils along the river flood plains (Fig. 1). The study region has continental climate with a mean annual precipitation of 350 mm (ranging from 400 to 700 mm) and mean temperature of -10^{o}C in January and 23^{o}C in July [11]. Lake Van (3713 km^2) is the largest lake of Turkey and located at an altitude of 1646 m above sea level. Lake Van, being a deep lake, does not freeze in winter due to its high salinity, except for its shallow northern section.

The lake has no outlet since active lava flows from Nemrut volcano that took place during Pleistocene block its westward outflow towards the Mus plain, the dormant Mount Nemrut closes western coastlines of the lake, and another dormant volcano Mount Suphan blocks its northern side. The water level in the lake fluctuates dramatically causing severe inundation of coastal vegetation, agricultural lands, and settlements. The study region includes Murat river and Karasu creek along with their river flood plains and three other lakes (Lakes Ercek and Nazik) to the east and west of Lake Van, respectively, and a crater lake on the top of the Mount Nemrut [3,8]. The study region has such main faults as Bitlis-Zagros fault zone (Bitlis thrust), Mus thrust, Karliova-Varto-Malazgirt, Karayazi-Tutak-Ercis, Tutak-Caldiran, Gevas, Suphan, Ahlat, Ozalp, Bahcesaray, Gurpinar, and Edremit faults.

Processing of ASTER Digital Elevation Model (DEM). According to Wilson and Gallant [12], and El Sheimy et al. [13], the methodological flow chart for the digital terrain characterization of the Lake Van region in terms of earthquake vulnerability is depicted in Fig. 2. ASTER sensor captures a comprehensive spectral spectrum ranging from visible to thermal-infrared and offer detailed spatiotemporal information on the earth surface conditions (e.g. vegetation, and geological features). ASTER DEM data were obtained from the Consortium for Spatial Information in the Geotiff format as 32 bit and were classified for the study region using both ArcGIS 10.2 [14] and Idrisi Taiga 16.03 [15]. The ASTER DEM data have the spatial resolution of 30 m with horizontal and vertical accuracies of 15 m and 8 m, respectively. The ASTER DEM data were used to classify DEM

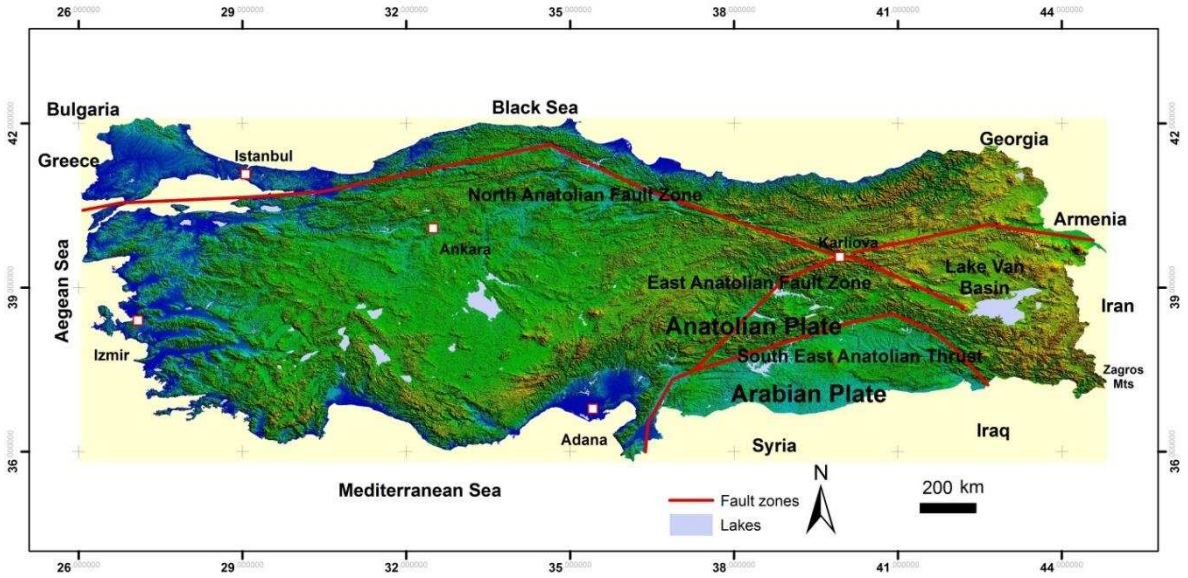

FIGURE 1
General information and location of the Lake Van region.

and to extract stream drainage patterns and lineaments of the study region. Before classification, using the Projection tool in ArcGIS 10.2, the DEM data were transformed from World Reference System geographic co-ordinates (λ, φ degrees) into the UTM projection system co-ordinates (in meters) with zone number 38N and the ED50 ellipsoid datum. The relevant DEM data were extracted according to the boundary frame of the Lake Van region using the Mask operation of the Extract tool in ArcGIS 10.2. The extracted DEM data were also imported to Idrisi Taiga for terrain classification and interpretation.

Landforms such as plains, plateaus, and mountains in the study region were demarcated using the ASTER DEM, and the GIS Analysis tools in Idrisi Taiga (Fig. 3 and Table 1). All the raster cells with the elevations from 500 to 1300 m were designated as low plains such as river flood plains after the interactive analysis of the DEM by the tool of Display Min/Max Contrast Setting in Idrisi Taiga. Elevations and abrupt changes in slopes and aspects were considered during the DEM classification. Elevations from 1300 to 1650 m were designated as plains; elevations from 1650 to 2200 m as plateaus; elevations from 2200 to 2500 m as mountains; and elevations from 2500 to 5150 m as high mountains (Figs. 3 and 4).

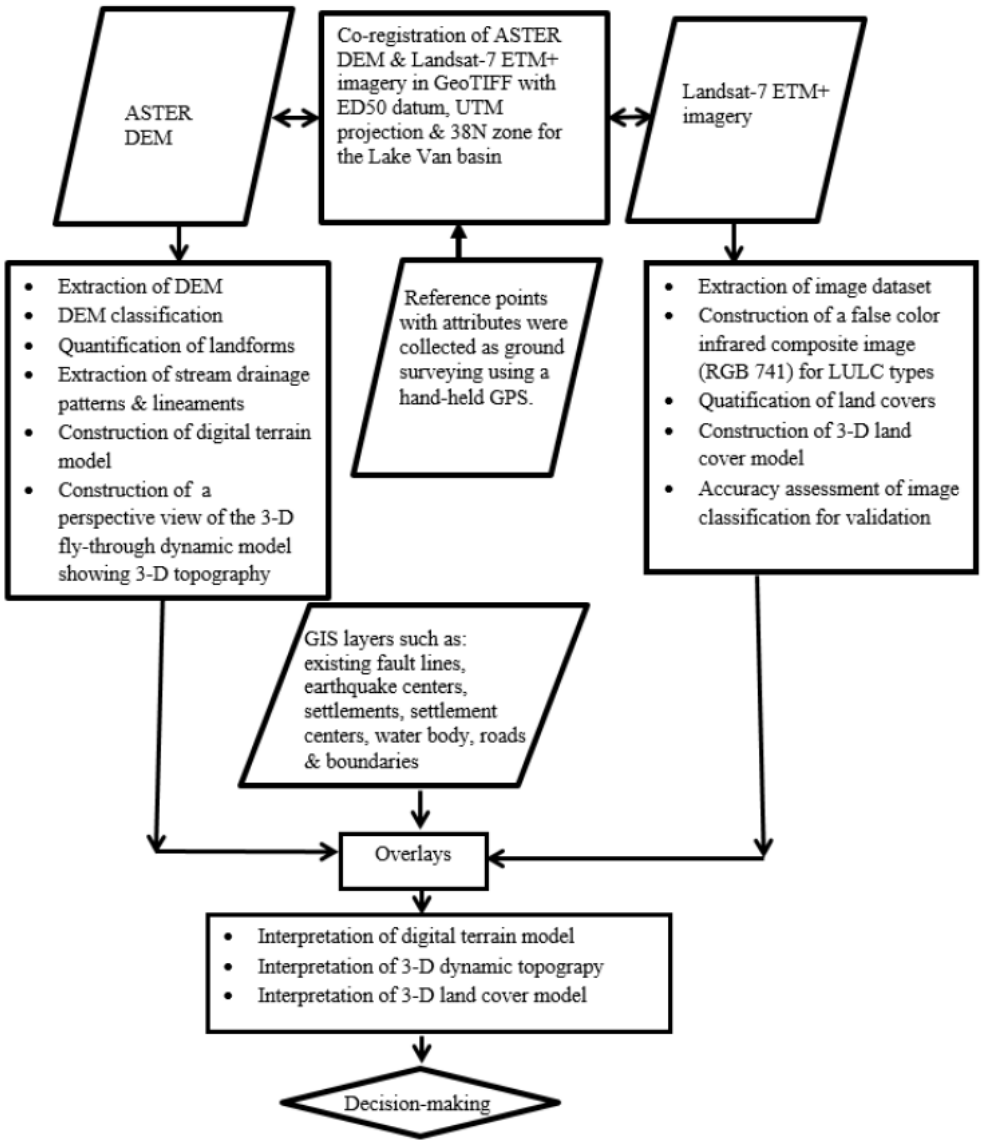

FIGURE 2
A flow chart of assessing vulnerability to earthquake hazard of the Lake Van region.

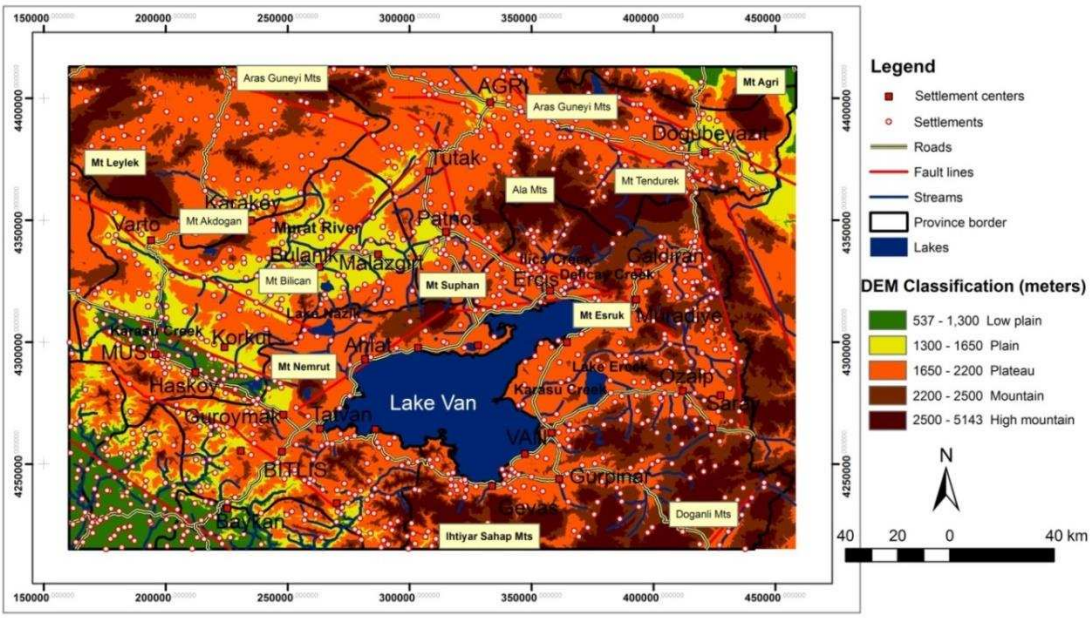

FIGURE 3
Quantification of geological landform structures of the Lake Van region.

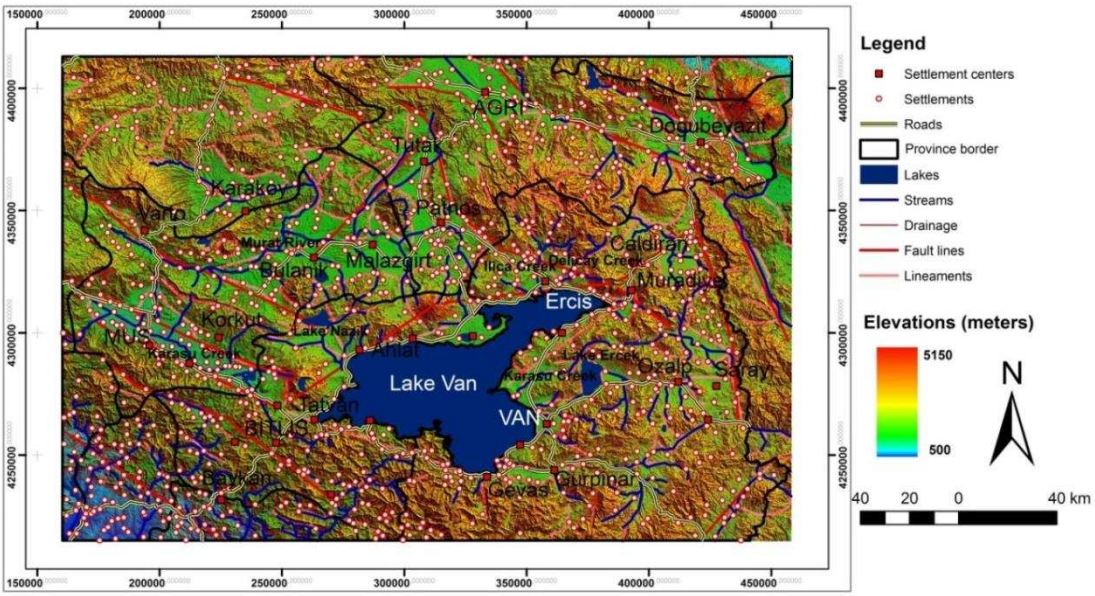

FIGURE 4
Digital terrain model of the Lake Van region showing lineaments as an indicator of faults and/or fractures, and stream drainage patterns.

TABLE 1
ASTER DEM-derived classification of the Lake Van region (grid size resolution = 30 m; horizontal accuracy = 15 m; and vertical accuracy = 8 m; elevation of Lake Van is 1646 m; and Mount Agri has the peak elevation of 5143 m).

DEM classification	Elevation (m)	Area (km^2)	Percent of total	Dominant land cover types (in decreasing order of magnitude)
Low plain	500–1300	1300	3.6	Agriculture/settlement/forest/water body
Plain	1300–1650	8650	23.7	Agriculture/settlement/water body/forest
Plateau	1650–2200	16500	45.2	Agriculture/settlement/bare rocks
Mountain	2200–2500	6150	16.8	Bare rocks
High mountain	2500–5143	3900	10.7	Bare rocks
Total area		36500	100	

Processing of Landsat-7 ETM+ multi-spectral imagery. A Landsat-7 ETM+ multi-spectral imagery geometrically and radiometrically rectified was obtained for July 2000 with path 171 and row 033 in World Reference System from the Global Land Cover Facility (GLCF), Earth Science Data Interface (ESDI). The Landsat-7 ETM+ imagery was used for the determination of LULC types of the study region. The Landsat-7 ETM+ provides a multi-spectral image data from eight spectral bands that have the spatial resolution of 30 m for the visible and near-infrared (bands 1-5 and 7) with the 15 m horizontal accuracy, of 15 m for the panchromatic (band 8) and of 60 m for the thermal infrared (band 6).

In this study, a false color infrared composite image (RGB 741) was first constructed from the Landsat-7 ETM+ imagery to visualize LULC types (Fig. 5). Near-infrared (NIR) band (band 4: 0.78–0.90 μm) of the Landsat-7 ETM+ was used to distinguish among water body, forest, settlement, agricultural land, and bare rock. A false color infrared composite image (RGB 741) was previously reported to be useful in distinguishing LULC types [16–18]. Using the Composite Tool in Idrisi, the infrared false color composite image was generated assigning band 7 to the Red (R) channel, band 4 to the Green (G) channel, and band 1 to the Blue (B) channel. Similarly, a standard infrared false color composite image (RGB 432), and a true color composite image (RGB 321) were generated to help to distinguish LULC types. The resultant composite images and the DEM classification were overlaid using Idrisi Taiga to qualitatively and quantitatively characterize and interpret earthquake vulnerability (Figs. 5 and 6).

Auxiliary digital maps and GIS data layers. Digital standard topographic maps of the study region at the scale of 1:100,000 were obtained from the Turkish General Command of Mapping. These digital maps include such auxiliary GIS data layers of the study region as settlements, settlement centers, housing, rivers, lakes, roads, and boundaries. These GIS layers as quadrangles were generated from the base maps of the standard topographic quadrangles at the scale of 1:100,000. Digital information about active fault lines was obtained from the General Directorate of Mineral Research and Exploration [19]. All these maps and GIS layers were used for geo-information, geo-referencing, overlaying, and comparing to the other resultant maps from the ASTER DEM and the Lansat-7 ETM+ imagery.

Digital terrain characterization for earthquake vulnerability. As was shown in Fig. 2 in the pre-processing stage, the ASTER DEM and the Landsat-7 ETM+ multi-spectral image data were co-registered in GeoTIFF format with a grid size of 30 m using the reference system of the ED50 ellipsoid datum and Universal Transverse Mercator (UTM) projection with zone number 38N. The boundary frame of the Lake Van region was extracted using the Mask operation of the Extract tool in ArcGIS, and imported to Idrisi for DEM classification, and the extraction and analyses of stream drainages and lineaments. Transformation for co-registration was carried out employing the Projection Tool in ArcGIS. The auxiliary GIS layers and the digital topographic maps at the scale of 1:100,000 were also used for geo-information and geo-referencing. In the process of decision-making about earthquake vulnerability of the study region, proximity to intersections of active fault-lines, distances to active fault-lines, historical earthquake backgrounds, structures of ground surface such as soft alluvial soils, liquefaction, rigid mountains, and volcanic and tectonic activities were considered in terrain characterization.

Digital terrain interpretation of stream drainage patterns and lineaments. To interpret DEM and landforms, the certain criteria were employed to obtain geo-information about the geological landforms in related literature [20–24]. For instance, color and color tones (attributes of height values) were used for DEM interpretation; topography and geomorphology (3D fly-through view and shaded DEM) for landform interpretation; and stream drainage patterns and lineaments for geo-structure derivation, in particular, lineaments, break-lines and fractures as an indicator of fault lines. In this study, ASTER DEM was used for the extraction of both drainage patterns and main lineaments which was in turn inputted to the analysis of geo-structures.

Shaded DEM, and DTM were used to extract geo-information (Fig. 4). This was particularly useful for extracting lineaments as well as analyzing the terrain. Jordan [25], and Jordan and Schott [26] explained how to extract lineaments from DEM. In their studies, the main lineaments were obtained by on-screen digitization from slope, aspect, shaded DEM, DEM segmentation, contours, curvatures, directional derivatives, and stream drainage patterns. Once all the digitized lineaments were combined, overlaid and analyzed, the meaningful lineaments were illustrated in Fig. 4. In so doing, settlement locations obtained from the standard topographical map at the scale of 1:100,000, stream drainage patterns, and lineaments were overlaid on the shaded ASTER DEM of the study region in ArcGIS. The terrain was visually interpreted with respect to geological structures, stream drainage patterns, and lineaments [18,23,24].

Generation of 3-D fly-through dynamic view. A 3-D fly-through view was generated

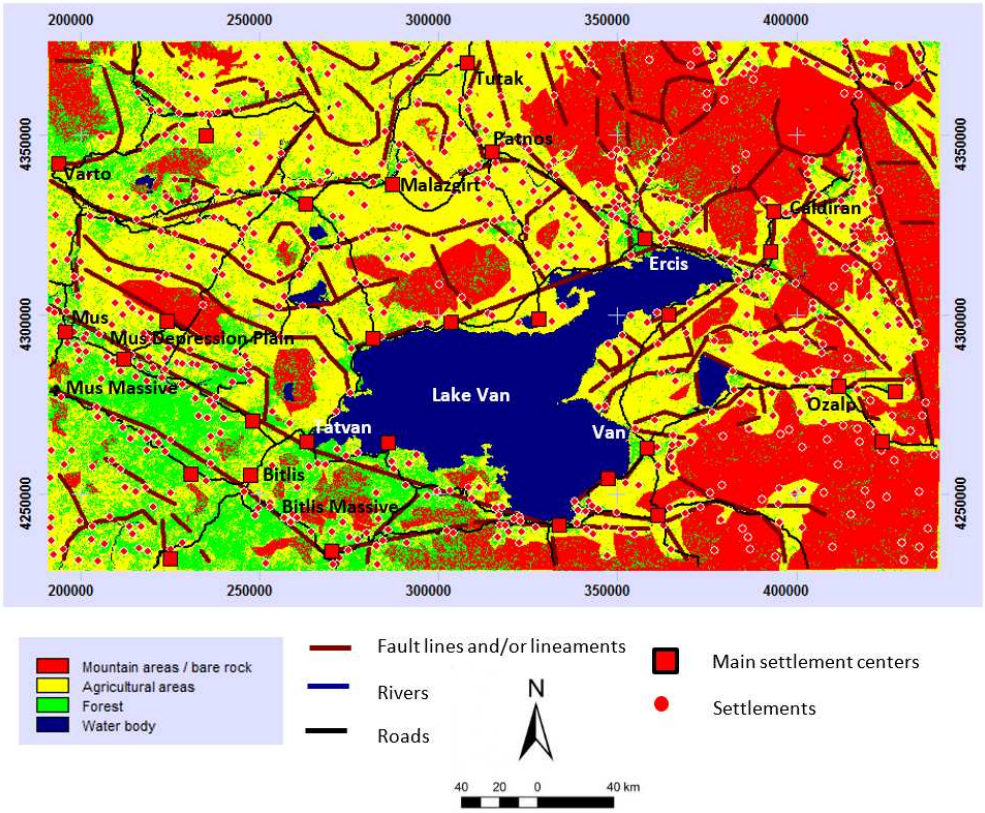

FIGURE 5
Land-use and land-cover (LULC) model of the Lake Van region.

draping LULC image and the false color infrared composite image (RGB 741) (Fig. 6) onto the original DEM data by using the fly-through tool in Idrisi Taiga. The 3-D LULC view generated (Fig. 6) is a dynamic model that allows for an interactive visualization of terrain characteristics with different vertical and horizontal scales and varying perspective views.

TABLE 2
Accuracy results for land-use and land-cover (LULC) model of the Lake Van region based on Landsat-7 ETM+ (July 2000) (grid size resolution = 30 m; horizontal accuracy = 15 m; PA = Producer's accuracy; and UA = User's accuracy).

LULC classification	PA (%)	UA (%)	Kappa	Area (km^2)	Percent of total
Agriculture	85	85	85	16500	45.2
Forest	95	95	95	6000	16.4
Settlement	85	85	85	500	1.4
Water body (lake/river)	98	98	98	3500	9.6
Bare rocks	85	85	85	10000	27.4
Total area				36500	100.0

RESULTS AND DISCUSSION

DEM classification provides information about slopes, aspects, elevations, drainage patterns, potential fault-lines, break-lines, volcanoes, and tectonic structures for a given study area. Lineaments as an indicator of fault-lines, horsts, grabens, and/or fractures were extracted from mountain borders, rises and depressions in terrain, ridges and valleys, break-lines, abrupt changes in slopes, scarps, and cliffs in DTM. DTM is useful for the determination of landforms such as agricultural soils, river flood plains, and rigid mountains and their suitability for settlements. The present study combines GIS and remote sensing techniques and interprets all the geographical data of different types, structures, formats, resolutions, accuracies and scales (spatial data of vectors and raster, and non-spatial data of textual attributes) in order to assist in the process of decision-making towards assessing earthquake vulnerability level of the Lake Van region and mitigating adverse impacts of potential earthquake damages.

Earlier studies focused on earthquake hazards only through the interpretation of DEM, topography, geological landforms, and faults overlaid with the spatial distributions of settlements. However, the novelty of the present study resides in the combined use of digital terrain characterization and interpretation of the study region for earthquake vulnerability by considering

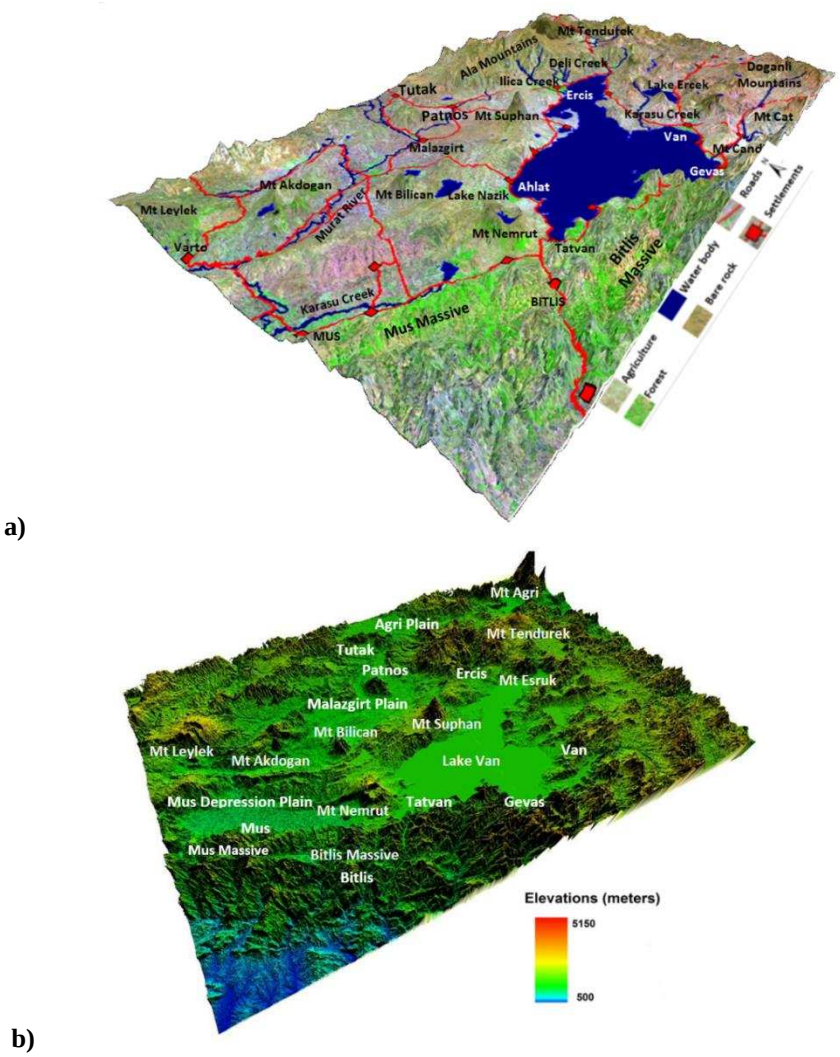

FIGURE 6
A three-dimensional (3-D) (a) land-use and land-cover (LULC) fly-through view and (b) DEM of the Lake Van region.

landforms, break-lines, stream drainage patterns, lineaments, and LULC types. DEM classification of the study region (36,500 km^2) consisted of low plains (3.6%), plains (23.7%), plateaus (45.2%), mountains (16.8%), and high mountains (10.7%) (Fig. 3) (Table 1). Our DTM (Figs. 3 to 6) indicates that the study region is composed mainly of plateaus (50 % of the study area), with different elevations and shapes over Tertiary sedimentary rocks and has volcanic massive to the west of Lake Van. The caldera complexes of Mounts Nemrut (2935 m), Suphan (4051 m), Esruk (2943 m), Tendurek (3298 m), Agri (5143 m) and Bilican (2950 m) are located around tectonically formed Lake Van.

Our LULC model classified the study region mainly under the five classes fairly well according to producer's and user's accuracies (Table 2). The DTM with the 3D fly-through dynamic view and the DEM classification allow for interpretation of earthquake vulnerability level by overlapping the settlements, active fault lines, earthquake locations with $M_w \geq 4.0$ since 1900, volcanic landforms, and geo-tectonic activities in the Lake Van region (Table 3). The earthquake vulnerability levels were based on the historical records of previous earthquakes provided by KOERI, distances between previous earthquake locations and the earthquake magnitudes, distances of the settlements to the main active fault lines and their intersections, and ground surface and/or earth crust factors such as rigid rocky areas, and alluvial soils prone to liquefaction (Table 3). This study reveals that all the coastal settlements around Lake Van are most vulnerable to earthquakes because of presence of soft soils in coastal plains, volcanic structures (Mt Nemrut, Mt Suphan, and Mt Esruk), active tectonic rigid structures, and active fault lines as the extension of the north Anatolian fault zone around the Lake Van. In addition, settlements over the Bitlis massive to the south of Lake Van where the Anatolian and the Arabian tectonic plates meet, and around Lake Ercek to the east of Lake Van show the highest vulnerability to potential earthquake damages.

TABLE 3
Vulnerability level assessment of the Lake Van region based on this study and the earthquake map of Turkey [2, 27–30].

Main settlements	Population (2016)	Earthquake vulnerability level	Fault lines/zones determined by remote sensing and GIS	Most severe earthquakes (M_w > 4) and years
Van	472,000	High	Van-Ozalp-Saray (Van fault)	4.7 (1968) 5.0 (1970) 7.2 (2011)
Ercis	174,000	High	Ercis-Patnos-Tutak (Ercis fault)	6.0 (1964) 5.0 (1976) 7.2 (2011)
Ipekyolu (Van Center)	285,000	High	Van-Ozalp-Saray (Van fault)	4.7 (1968) 5.0 (1976) 7.2 (2011)
Tusba (Van Center)	150,000	High	Van-Ozalp-Saray (Van fault)	4.7 (1968) 5.0 (1970) 7.2 (2011)
Edremit	119,000	Medium	Bitlis thrust	-
Ozalp	70,000	High	Van-Ozalp-Saray (Van fault)	4.9 (1962) 6.0 (1972)
Saray	22,000	Low	Van-Ozalp-Saray (Van fault)	-
Muradiye	51,000	High	Muradiye-Caldiran-Dogubeyazit (Caldiran fault)	4.6 (1952) 7.0 (1976)
Caldiran	66,000	High	Muradiye-Caldiran-Dogubeyazit (Caldiran fault)	7.3 (1976) 4.7 (1977)
Gevas	29,000	Medium	Bitlis thrust	4.6 (1966) 4.3 (1974)
Çatak	22,000	High	Bitlis thrust	5.8 (1945) 4.9 (1961)
Bahcesaray	16,000	Medium	Bitlis thrust	-
Baskale	56,000	Medium	Bitlis thrust	4.3 (1947)
Gurpınar	37,000	Medium	Bitlis thrust	4.8 (1951) 4.9 (1972)
Bitlis	67,000	Medium	Bitlis thrust	4.9 (1963) 4.5 (1964) 4.5 (1966)
Tatvan	89,000	Medium	Bitlis thrust	4.6 (1941) 4.5 (1945) 4.5 (1960)
Mutki	32,000	High	Bitlis thrust	5.8 (1960)
Hizan	36,000	High	Bitlis thrust	4.3 (1963) 5.0 (1966)
Guroymak	46,000	Medium	Mus thrust (Mus-Bitlis Massive)	-
Adilcevaz	31,000	Medium	Guroymak-Ahlat-Adilcevaz (Nemrut and Suphan faults)	4.6 (1959)
Ahlat	39,000	Medium	Guroymak-Ahlat-Adilcevaz (Nemrut and Suphan faults)	4.3 (1957)
Siirt	156,000	High	Bitlis thrust	5.2 (1947) 5.5 (1960) 4.9 (1964)
Baykan	27,000	High	Bitlis thrust	-
Mus	189,000	High	Mus thrust (Mus-Bitlis Massive)	5.3 (1953) 5.3 (1966) 4.3 (1968)
Haskoy	27,000	High	Mus thrust (Mus-Bitlis Massive)	-
Korkut	26,000	High	Mus thrust	-
Varto	31,000	High	Varto-Bulanik-Malazgirt (Malazgirt fault)	5.8 (1950) 6.1 (1966) 5.2 (1969)
Bulanik	82,000	High	Varto-Bulanik-Malazgirt (Malazgirt fault)	6.0 (1936)
Malazgirt	54,000	High	Varto-Bulanik-Malazgirt (Malazgirt fault)	5.2 (1907)
Agri	149,000	High	Agri-Dogubeyazit (Dogubeyazit fault)	5.8 (1941) 4.5 (1967)
Tutak	32,000	High	Ercis-Tutak-Karayazi (Tutak fault)	-
Patnos	125,000	High	Ercis-Tutak-Karayazi (Tutak fault)	5.2 (1941) 5.5 (1952) 4.6 (1964)
Dogubeyazit	122,000	High	Agri-Dogubeyazit (Dogubeyazit fault)	5.0 (1946) 5.0 (1962)
Hamur	20,000	High	Agri-Dogubeyazit (Dogubeyazit fault)	5.6 (1936)

As a result of the interpretation of the color composite images, the study region appears to have limited patches of forests and agriculture except for the districts of Karasu creek and Murat river flood plains in Mus. The study region is mostly covered with pastures and grasslands which in turn led to the development of livestock and husbandry. Some scattered forest areas exist on the mountains of Mus and Bitlis. All the volcanos and most of the high mountains have bare rocks except for Bitlis massive covered with forest (Fig. 5). The interpretation of Figs. 5 and 6 along with field works shows that the agricultural plains and plateau plains are dominantly used for growing grains, and to a small extent, for orchards, especially along the Murat river and Karasu creek flood plains.

The settlements in the low flood plains of Mus, Malzagirt, and Korkut have the highest flooding risk due to Murat river, and Karasu creek. The Mus plain has connectivity with the drainage systems of Murat and Euphrates (Firat) rivers (Figs. 3 to 6). Lineament analysis may be used to assess earthquake risk levels by determining fractures with vertical or horizontal shifts in the rocks on either side of the fault. The lineaments determined in the study region are of different dimensions, orientations, distributions, and relationships among themselves (Fig. 4). Our lineament analysis revealed that the Mus and southeastern Anatolian thrusts between the Anatolian and Arabian plates along the Ercis-Van-Gevas-Tatvan-Mus direction, and the eastern extension of the north Anatolian fault zone along the Ercis-Patnos-Malazgirt-Varto-Karliova direction have low plains with sedimentary alluvium soils, and thus, have the highest level of earthquake risk. Though outside of the study region, Karliova is also an important junction where the north and east Anatolian fault zones intersect.

The eastern parts of Lake Van as a water accumulation area appear not to be safe for settlements due to their soft ground. Not only should the approach for DTM in the present study be integrated with the processes of public policy- and decision-making and land-use planning across Turkey, but also precautionary measures should be taken to orient the sprawl and development of settlements away from the earthquake risk areas determined in the study region. In order for major earthquake disasters such as the most recent event not to be re-experienced somewhere else in a similar way, DTM-assisted land-use planning regarding the selection of alternative settlement areas that could withstand future earthquakes comes to the forefront for a pre-earthquake disaster prevention prior to ensuring the abilities to construct buildings to current standards of seismic resistance to avoid structural failure and to take emergency preparedness measures to minimize pain and loss of life.

Local processes of transformation and translocation of rural environment to growing urban agglomerations have occurred globally at unprecedented rates, and thus, call for mapping, monitoring and assessing earthquake prone regions and their seismic vulnerability levels, as with the present study. For example, Geiß et al. [31] based their spatiotemporal estimates of seismic vulnerability levels of urban structures in the earthquake-prone mega city of Istanbul on multispectral RapidEye and Landsat archive datasets, and elevation data from the TanDEM-X mission. Similar techniques were also used successfully in related literature [32–34].

CONCLUSIONS

In conclusion, a simple methodology for DTM was devised to visualize geo-information and to quantify terrain characteristics to assist in the process of decision-making for the protection of the study region against potential earthquake hazards. DTMs can be extended to the characterization and interpretation of a wide range of other natural hazards such as flooding, fires, landslides, storms, and volcanic eruptions. Whether land suitability assessment is involved in the selection of appropriate residential, commercial, industrial, disposal or energy facility sites, DTMs play an important role in the formulation of sustainable public policies. Analyses of DTM accuracy and precision depend on the spatiotemporal and radiometric resolutions of the satellite- or radar-derived DEM and imageries, uncertainty and sensitivity analyses, processing errors with geo-referencing, transformation of map projection, digital terrain analyses, quality control and quality assurance of both in situ and remote sensing measurements, and the integration of remote and proximal sensors and field campaigns. In addition to multispectral sensors, the other active and passive remote sensing tools such as Light Detection and Ranging (LiDAR) and hyperspectral sensors remain to be explored for spatiotemporal mapping and monitoring of vulnerability level and vulnerability mitigation (e.g. security, and emergency preparedness) of not only urban but also rural seismic areas in the face of urbanization processes.

ACKNOWLEDGEMENTS

Izmir Institute of Technology and Abant Izzet Baysal University are gratefully acknowledged for the financial and logistical supports.

REFERENCES

[1] EM-DAT. (2015) The OFDA/CRED International Disaster Database. Available online: http://www.emdat.be (accessed on 26 January 2015).

[2] Korkmaz, K.A. (2009) Earthquake disaster risk assessment and evaluation for Turkey. Environ. Geol. 57, 307–320.

[3] Saroglu, F., Emre, O. and Kuscu, I. (1992) Active Fault Map of Turkey. General Directorate of Mineral and Research Exploration of Turkey Publication.

[4] Utada, H. (1993) On the physical background of the Van earthquake prediction method. Tectonophysics, 224, 153–160.

[5] Zor, E., Gurbuz, C., Turkelli, N., Seber, D. and Barazangiet, M. (2003) The crustal structure of the east Anatolian plateau from receiver functions. Geophys. Res. Lett. 30, 8044.

[6] Utkucu, M. (2006) Implications for the water level change triggered moderate (M >= 4.0) earthquakes in Lake Van basin, eastern Turkey. J. Seismol. 10, 105–117.

[7] Horasan, G. and Guney, A.B. (2007) Observation and analysis of low-frequency crustal earthquakes in Lake Van and its vicinity, eastern Turkey. J. Seismol. 11, 1–13.

[8] Pinar, A., Honkura, Y., Kuge, K., Sezgin, N., Yilmazer, M. and Ogutcu, Z. (2007) Source mechanism of the 2000 November 15 Lake Van earthquake (Mw =5.6) in eastern Turkey and its seismotectonic implications. Geophys. J. Int. 170, 749–763.

[9] Selcuk, L., Selcuk, A.S. and Beyaz, T. (2010) Probabilistic seismic hazard assessment for Lake Van basin, Turkey. Nat. Hazards 54, 949–965.

[10] Birkmann, J (Ed.). (2006) Measuring vulnerability to natural hazards: towards disaster resilient societies. United Nations University Press.

[11] General Directorate of Meteorology. Climate Assessment. (2015) Available online: http://www.mgm.gov.tr/veridegerlendirme/yagis-raporu.aspx (accessed on 26 September 2015) (in Turkish).

[12] Wilson, J.P. and Gallant, J.C. (2000) Terrain analysis: principles and applications. John Wiley and Sons, New York, 2000.

[13] El Sheimy, N., Valeo, C. and Habib, A. (2005) Digital terrain modeling: acquisition, manipulation and applications. Artech House, Boston.

[14] ArcGIS. ArcGIS 10.2. Redland, CA: ESRI.

[15] Idrisi. Idrisi Taiga 16.03. Clark University, Clark labs, Worcester, MA.

[16] Lillesand, T.M. and Kiefer, R.W. (2004) Remote sensing and image interpretation. John Wiley and Sons, New York.

[17] Jensen, J.R. (2005) Introductory digital image processing: a remote sensing perspective (3rd Ed.). Prentice-Hall, New Jersey.

[18] Demirkesen, A.C. (2008) Digital terrain analysis using Landsat-7 ETM+ imagery and SRTM DEM: a case study of Nevsehir province (Cappadocia), Turkey. Int. J. Remote Sens. 29, 4173–4188.

[19] General Directorate of Mineral Research and Exploration. (2014) Active Fault Map of Turkey. Available online: http://www.mta.gov.tr/v2.0/eng/index.php (accessed on 26 December 2014) (in Turkish).

[20] Prost, G.L. (1994) Remote sensing for geologists: a guide to image interpretation. Taylor and Francis, London.

[21] Florinsky, I.V. (1998) Combined analysis of digital terrain models and remotely sensed data in landscape investigations. Prog. Phys. Geog. 22, 33–60.

[22] Konecny, G. (2002) Geoinformation: remote sensing, photogrammetry and geographical information systems. Taylor and Francis, London.

[23] Demirkesen, A.C. (2009) Quantifying geological structures of the Nigde province in central Anatolia, Turkey using SRTM DEM data. Environ. Geol. 56, 865–875.

[24] Demirkesen, A.C. (2012) Multi-risk interpretation of natural hazards for settlements of the Hatay province in the east Mediterranean region, Turkey using SRTM DEM. Environ. Earth Sci. 65, 1895–1907.

[25] Jordan, G. (2003) Morphologic analysis and tectonic interpretation of digital terrain data: a case study. Earth. Surf. Processes 28, 807–822.

[26] Jordan, G. and Schott, B. (2005) Application of wavelet analysis to the study of spatial pattern of morphotectonic lineaments in digital terrain models: a case study. Remote Sens. Environ. 94, 31-38.

[27] AFAD. (2016) Disaster and Emergency Management Presidency, Earthquake Department. Available at http://www.deprem.gov.tr/sarbis/Shared/Default.aspx (in Turkish)

[28] KOERI. (2016) Kandilli Observatory Earthquake Research Institute. Integrated homogeneous Turkey's Earthquake Catalog. Available at http://www.koeri.boun.edu.tr/sismo/ (in Turkish)

[29] TUIK. (2016) Turkish Statistical Institute. Available at http://www.turkstat.gov.tr (in Turkish)

[30] Tabban, A. (2000) Geology of cities and earthquake condition. The Chamber of Geology Engineering, Publishing no: 56, Ankara (in Turkish).

[31] Geiß, C., Jilge, M., Lakes, T. and Taubenböck, H. (2016) Estimation of seismic vulnerability levels of urban structures with multisensor

remote sensing. IEEE J. Sel. Top. Appl. Earth Obser. Remote Sens. 9, 1913-1936.
[32] Seker DZ., Kaya S., Alkan RM., Tanik A. and Saroglu E. (2008) 3D coastal erosion Analysis of Kilyos-Karaburun region using multi-temporal satellite image data. Fresen. Environ. Bull. 17, 1977-1982.
[33] Coskun HG. (2009) Remote sensing and GIS techniques for temporal evaluation of environmental impacts on major drinking water dam and basin of metropolis Istanbul. Fresen. Environ. Bull. 18, 261-273.
[34] Donmez C., Berberoglu S., Cilek A. (2016) Understanding spatial and temporal snow dynamics of a Mediterranean catchment using process-oriented modelling and remote sensing. Fresen. Environ. Bull. 25, 1609-1622.

Received: **26.08.2016**
Accepted: **25.01.2017**

CORRESPONDING AUTHOR

Fatih Evrendilek
Abant Izzet Baysal University Faculty of Engineering & Architecture Department of Environmental Engineering 14280 Golkoy Campus, Bolu – TURKEY

e-mail: fevrendilek@ibu.edu.tr